NASA TECHNICAL MEMORANDUM

NASA TM X-71827

NASA TM X-71827

(NASA-TM-X-71827) ACCUSTIC SYSTEMS CONTAINING CUFVED DUCT SECTICNS (NASA) 22 p HC $3.50 CSCL 20A

N76-13881

Unclas

G3/71 05367

ACOUSTIC SYSTEMS CONTAINING CURVED DUCT SECTIONS

by W. Rostafinski
Lewis Research Center
Cleveland, Ohio 44135

TECHNICAL PAPER presented at
Ninetieth Meeting of the Acoustical
Society of America
San Francisco, California, November 4-7, 1975

E-8458

ACOUSTIC SYSTEMS CONTAINING CURVED DUCT SECTIONS

by W. Rostafinski

National Aeronautics and Space Administration

Lewis Research Center

Cleveland, Ohio 44135

ABSTRACT

The analysis of waves in bends in acoustical ducting of rectangular cross section is extended to the study of motion near discontinuities. This includes determination of the characteristics of the tangential and radial components of the non-propagating modes. It is established that attenuation of the non-propagating modes strongly depends on frequency and that, in general, the sharper the bend, the less attenuation may be expected. Evaluation of a bend's impedance and of impedance-generated reflections is also presented in detail.

INTRODUCTION

Rectilinear acoustic systems consisting of sections of straight, hard-walled ducts of different diameters, or containing aperatures and similar constrictions, are characterized by propagation parameters independent of frequency which can be described by relatively simple relations. Unfortunately, formulations derived for straight lines are inadequate for acoustic systems containing curved sections. The basic reason for this is that curved ducts constitute a dispersive medium; in other words, wave velocity in bends is a function of the frequency. While in a straight duct only non-rigid walls create a dispersive medium for the progressing wave in its basic plane wave mode, in curved duct sections the zeroth mode will depend on frequency even with rigid walls and must be treated accordingly. The reason for this lies in the inability of curved ducts to carry plane waves. A plane wave at the inlet of the bend will become non-plane in the bend; for that matter, it begins to change to non-plane already in the straight duct feeding the bend. Consequently, in the bend, besides the progressing tangential component of particle velocity there will be more or less pronounces radial oscillations. The well-known illustration of the nature of plane waves advancing in tubes involves imagining an axial partition inside the tube. Insertion of such a partition in a straight duct will not modify the parameters of a plane wave. In a bent section, however, a partition concentric with the curved side walls will completely modify the original distribution of velocities and pressures. It will also affect the level of radial oscillations. The reason for this is that a partition forms two concentric bends less sharp than the original bend and creates essentially new boundary conditions.

In previous investigations of the characteristics of waves moving in curved bends(1, 2) it was demonstrated that propagation in cylindrical bends, away from any discontinuity, is characterized by a lack of backwards reflections resulting from curvature of the walls. Only onwards reflections are present. This very basic result of analytical work was recently verified experimentally by Cummings.(3) On the other hand, in duct systems containing bends, the propagating waves will be accompanied by non-propagating modes originating at discontinuities. In Ref. 1 the evanescent waves appearing at junctions between a straight duct and a cylindrical bend were studied in great detail (using an exact solution of the wave equation), but analysis was limited to long waves and very low frequencies. In a subsequent study (Ref. 2), higher frequencies and higher modes were considered, but in the steady state only; non-propagating evanescent waves requiring the use of imaginary-order Bessel functions were left out. The problem, however, is that the description of the motion of waves in duct systems cannot be complete without some understanding of the nature and extent of the non-propagating modes, which, as will be shown, may propagate quite far along the curved duct before dying out. It will also be shown that the non-propagating modes significantly modify the acoustic field at the bend's inlet. Thus far, the basic mode in hard-walled ducting has been investigated quite extensively (Ref. 2). The results yield a good understanding of motion in typical industrial ducting. The higher modes have been given some attention but in view of the predominant role of the lowest mode and of its exclusivity in a relatively wide range of low frequencies, the higher modes seem to be of lesser importance in engineering. In most cases the higher modes, if at all excited, will belong to the evanescent, non-propagating category. Consequently, in Ref. 4 energy flow in curved ducts was analyzed in the basic mode only. The conclusion of this work was that an important attenuation of sound should be expected in sharp bends.

This paper will give the results of an analysis of the changes that occur as waves move in curved cylindrical ducting. The physical system considered uses cylindrical coordinates (r, θ) and consists of a two dimensional circular bend with inner- and outer-wall radii R_1 and R_2 respectively. The walls are assumed perfectly rigid. The bend is connected to a straight duct forming a discontinuity at the junction. For study of the non-propagating modes a vibrating piston will be substituted for the straight duct. The important subject of a bend's acoustic impedance and impedance-generated reflections will be developed in some detail. Except for the solution of the characteristic equation for finding roots, the entire analysis is an exact solution of the wave equation.

The Non-Propagating Modes

In the study of the long waves that is for $kR_1 << 1$, (Ref. 1), using a simplified series expression of the characteristic equation of wave motion in bends

$$J'_{\nu_m}(akR_1)J'_{-\nu_m}(kR_1) - J'_{-\nu_m}(akR_1)J'_{\nu_m}(kR_1) = 0 \qquad (1)$$

where $akR_1 = kR_2$, it was possible to determine the single real root ν_0 yielding the propagating mode, as well as the infinite set of pure imaginary roots

$$\nu_m = m\pi i/\ln a \qquad m = 1, 2, 3, . . . \qquad (2)$$

corresponding to the non-propagating, evanescent modes.

The evaluation of the motion of waves of higher frequencies (Ref. 2) was based on closed form solutions of the Bessel equation corresponding to orders $\nu_m = (m + 1/2)$, $m = 1, 2, 3, ...$

This type of approach, however, does not allow for determination of the imaginary roots. Instead use must be made of special expressions for Bessell functions of imaginary order $\nu_m = i\mu_m$. Such series, first published in 1844 by Boole[5], were given in a more convenient form, and tabulated, by Buckens[6] in 1963. Because of the little-known form of these series, they will be given here for convenience.

Bessel functions of a purely imaginary order and of real argument are solutions of the equation

$$x^2\varphi'' + x\varphi' + (x^2 + \mu^2)\varphi = 0$$

The fundamental pair of solutions is defined by

$$F_\mu = A_\mu(x) \cos(\mu \ln x) - B_\mu(x) \sin(\mu \ln x)$$

$$G_\mu = A_\mu(x) \sin(\mu \ln x) + B_\mu(x) \cos(\mu \ln x)$$

where

$$A_\mu(x) = \sum_{n=0} a_{2n}(ix)^{2n}$$

$$B_\mu(x) = \sum_{n=0} b_{2n}(ix)^{2n}$$

and a and b are given by recurrence formulae

$$a_{2n} = \frac{na_{(2n-2)} + \mu b_{2n-2}}{4n(\mu^2 + n^2)}$$

$$b_{2n} = \frac{nb_{(2n-2)} - \mu a_{(2n-2)}}{4n(\mu^2 + n^2)}$$

with $a_o = 1$ and $b_o = 0$.

The most general solution of the wave equation in cylindrical coordinates (using $kr = x$) is

$$\phi = \sum_m \varphi_m(kr) \exp i(\omega t - \nu_m \theta)$$

where, with Bessel functions of pure imaginary order but of real argument

$$\varphi_m(kr) = A_m G_\mu(kr) + B_m F_\mu(kr)$$

Differentiating $\varphi_m(kr)$ with respect to the argument along with a rigid wall boundary condition, gives

$$G'_\mu(akR_1) \cdot F'_\mu(kR_1) - G'_\mu(kR_1) \cdot F'_\mu(akR_1) = 0 \qquad (3)$$

This characteristic equation of motion of the non-propagating modes parallels equation 1. For very low frequencies, this characteristic equation yields the roots given by Eq. 2, derived in Ref. 1. For higher values of kR_1, however, the roots do not fit into such a simple relation. These roots have been evaluated on a digital computer by programming Eq. 3. The program iteratively locates and converges to the roots (eigenvalues) of Eq. 3. The convergence criterion is accuracy to the eighth decimal place.

The program is not long nor complicated. Because of its simplicity it can be written readily for any specific application. Here, for illustrative purposes only, two curved ducts characterized by $a = R_2/R_1 = 2$ and 4 have been analyzed and the results are given in Figs. 1 and 2. For the duct with $a = 2$, the roots can be approximated by Eq. 2 for $kR_1 < 1$. With higher frequencies the first root becomes very small, vanishing at $kR_1 = \pi$. The next root ($m = 2$) vanishes at $kR_1 = 2\pi$.

For a = 4 the root pattern is very similar but the small root zone is shifted to lower frequencies and all roots are smaller than in the case of a = 2. Approximate values of the roots for ducts with a = 4 can be calculated by Eq. 2 provided that $kR_1 < 0.5$.

As a consequence of the appearance of small roots μ_m in the solution of the wave equation for non-propagating modes, the term $\exp(-\mu\theta)$ will remain unattenuated until θ grows to large values such as π or greater. In other words there exist frequency ranges in which the non-propagating waves will be pronounced even well downstream from discontinuities and the steady state distribution may not be reached in typical industrial bends of 45^{o} or 90^{o}. In such bends, the distribution of particle velocities and of pressure cannot be predicted unless the evanescent waves are taken into consideration. Because with increasing "a" the general level of roots decreases, the sharper a bend the more the non-propagating modes will be sustained in their existence. Furthermore, since the evanescent waves may propagate far into the bend, any wall treatment designed to eliminate or reduce noise must be carefully designed to be effective: All depends on the degree of attenuation on non-propagating modes. At frequencies at which the non-propagating modes tend to propagate far into the bend, the higher propagating modes will appear if excited.

To illustrate the point, propagation parameters have been calculated for a bend with radii a = 2 and for waves with frequencies corresponding to waves characterized by Bessel functions of order (m + 1/2) for m ranging from 0 to 6. The propagating modes of these waves were described in Ref. 2. It may be worthwhile to restate here the values of the parameters of these waves for the lowest propagating mode:

ν_m	0.5	1.5	2.5	3.5	4.5	5.5	6.5
kR_1	0.3396	1.0115	1.6633	2.2869	2.8817	3.4523	4.0065

The calculated non-propagating, tangential and radial, vibrational velocities at two tangential positions: at $\theta = \pi/64$, that is, very close to the surface of the piston generating waves at the bend's inlet, (and therefore in the region of discontinuity), and at $\theta = \pi/4$; are shown on Figs. 3 and 4. The vibrational velocities are nondimensionalized using v_0, the vibrational velocity of the piston. For clarity in Fig. 3 the tangential waves are shown in three plots. In the range of low frequencies, for $kR_1 < 1.6633$, the distribution of velocities near the piston is nearly that of a potential vortex but the attenuation is fast and by $\pi/4$ the vibrations become insignificant, reduced by two orders of magnitude. The case of $kR_1 = 2.2869$ is a particular case of very small vibrations throughout the bend, of unusual distribution and of very satisfactory attenuation. At frequencies corresponding to $kR_1 > \pi$, the attenuation is again very fast. The evanescent, radial vibrational velocities are shown in two plots - Fig. 4. For frequency parameters $kR_1 < 2.2869$ the radial oscillations are relatively small and attenuate fast, reaching negligibly small amplitudes by $\pi/4$. At higher frequencies (except for $kR_1 = 2.8817$) the radial component is even less pronounced, and it attenuates very fast. It will also be noticed that the radial evanescent waves may be either positive or negative, depending on the frequency range.

Figure 5 gives the tangential vibrational velocities v_θ for three angular positions: at $\pi/64$, close to the piston, at $\pi/8$, and at $\theta = \infty$. Data for $v_\theta = \infty$ were taken from Ref. 2. The values of v_θ at $\pi/64$ and $\pi/8$ were calculated by adding to (or subtracting from) $(v_\theta)_\infty$ values of the $(v_\theta)_{evanescent}$ similar to those given on Fig. 3. Except for the case of frequency parameter $kR = 2.8817$, v_θ acquires its final distribution relatively fast in duct cross sections. At $\pi/64$ the distribution is quite pronounced near the two curved walls of the bend, but in the central part of the bend's cross section $v_\theta = 1$, as it should be. However, at $kR_1 = 3.4523$, where the first root of the characteristic equation has already vanished, the distribution of v_θ for all θ seems to be very close to the final distribution at $\theta = \infty$.

Acoustic pressure variations in the bend's cross sections are shown on Fig. 6. The data are nondimensionalized using p_o the acoustic pressure at piston corresponding to vibrational velocity v_o. The first two graphs, pertaining to very low frequencies, indicate a very uniform pressure distribution near the piston's face. At all other frequencies the variation of pressure with the radius is pronounced. For $kR_1 = 3.4523$ attenuation of the non-propagating modes takes place at $\theta < \pi/64$.

The variation of pressure in the bends, as shown, cannot be calculated using information on tangential velocity distribution except for very low frequencies corresponding to $kR_1 << 1$, because the solution of the wave equation in evanescent modes is a series solution. Each term of the series pertains to its m'th root and has its own integration constant. Only when the first term of the expansion yields a satisfactory solution, as in the case of the very low frequencies, is such direct recalculation permitted. The calculated distribution of pressure in bends matches well, in its general geometry, the experimental data of Cummings[3].

The Bend's Acoustic Impedance and Transmission

The specific acoustic impedance of duct bends

$z = \rho c(kR_1/\nu_m)(r/R_1)$

has been derived in Ref. 2. This quantity, integrated and averaged over the duct's cross section (of unit depth) gives

$z_c = \rho c(kR_1/2\nu_m)(a + 1) = \rho c'$

where the index c indicates that the expression refers to the cross section's area, and where c' is the phase velocity of the progressive wave at the bend's centerline, as derived in Ref. 1. The dimensionless impedance for a duct of unit depth is defined by

$$z_n = (kR_1/2\nu_m)(a + 1) = c'/c \quad (4)$$

The z_n have been calculated for the lowest propagating mode and for several duct parameters $a = R_2/R_1$ and for a range of frequencies, and the results have been plotted on Fig. 7. Values of z_n for a relatively narrow duct ($a = 1.5$) are very close to unity, indicating that the specific acoustic impedance of a duct of low aspect ratio is nearly the same as the specific acoustic impedance of a straight tube ($z_c = \rho c$) and consequently is independent of frequency. All other characteristics on Fig. 7 become progressively steeper with increasing parameter a, that is, with increasing sharpness of bends. However, there is always one particular value of the frequency paramater kR_1 at which $z_c = \rho c$ in spite of the fact that the waves at these frequencies are far from being plane. In connection with this, it will be noted in Ref. 2 that at some frequency, distribution of tangential vibrational velocity shows a minimum of distortion at a frequency approximately corresponding to $z_c = \rho c$. The consequence of z_c being generally different from ρc will show itself in the sound-transmitting ability of bends.

Assume waves advancing in two directions of θ, the incident and the reflected wave trains. Expressions describing these waves, the acoustic pressure and the tangential velocity, are:

$$p = -\rho\ \partial\phi/\partial t = +\rho ikc[A_i e^{-\nu\theta} - A_r e^{\nu\theta}]F(kr)e^{i\omega t}$$

$$v_\theta = 1/r\ \partial\phi/\partial\theta = +i\nu[A_i e^{-\nu\theta} + A_r e^{\nu\theta}]F(kr)/re^{i\omega t}$$

where F(kr) stands for the function of radial dependence of motion under consideration. A similar set of equations can be written for propagation of the transmitted wave in a straight duct connected to the bend. In this second set of equations $\nu\theta$ must be replaced by kx and the expression for the axial velocity by $v_x = \partial\phi/\partial x$. The condition of continuity of pressure and velocity at the junction between the bent (incident and reflected waves) and the straight (the transmitted wave) ducts at $\theta = x = 0$, (both assumed extending to infinity to simplify somewhat the model) is

$$\left.\frac{p_{prop} + \sum_j p_{nonprop}}{v_{\theta\, prop} + \sum_j v_{\theta\, nonprop}}\right|_{\theta=0} = \sum_j \left(\frac{p}{v_x}\right)\Bigg|_{x=0} \tag{5}$$

where p and v include the incident and the reflected waves. Now, evaluating the numerator and the denominator of the left hand side of Eq. 5, written in the form

$$p_{prop}(1 + p_1/p_{prop} + p_2/p_{prop} + \ldots .)$$

it is verified that the variable terms in the parentheses decrease with frequency and become very small at low frequencies. Consequently Eq. 5 gives, for $\sum_j \left(\frac{p}{v_x}\right) \rho c$,

$$(kr/\nu)(A_i - A_r)/(A_i + A_r) = 1$$

which, integrated and averaged over the cross section of the bend, yields

$$(kR_1/2\nu)(a + 1)\ (A_i - A_r)/(A_i + A_r) = 1$$

or

$$z_n(A_i - A_r)/(A_i + A_r) = 1$$

Now, the ratio of the amplitude of the reflected wave to the amplitude of the incident wave, that is, amplitude reflection coefficient r, is

$$r = A_r/A_i = (z_n - 1)/(z_n + 1) \tag{6}$$

and the sound reflection coefficient $\alpha_r = r^2$, while the sound transmission coefficient will be $\alpha_t = 1 - \alpha_r$.

In the case of two bends (numbers 1 and 2) of different curvatures, but of the same cross section, and connected in series:

$$r = \left({}_1z_n - {}_2z_n\right) / \left({}_1z_n + {}_2z_n\right)$$

The standard form of the standing wave radio SWR = (1 + r)/(1 - r) as derived for straight ducts and pipes applies here without change. Physically, the situation is analogous to the acoustic phenomena at the boundary of two media. Equations 4 and 6 allow us to calculate reflections at the boundary between a "dense medium" (bend) and a "less dense medium" (straight duct), or vice versa, depending on frequency. These reflections depend, of course, on the sharpness of the bend (parameter a). For the great majority of bends met in industrial applications, they will be quite low. Reflections appear because the impedance of curved ducts is different from the impedance of straight lines of the same cross section. For analytical purposes a straight duct-bend system can be replaced, as far as transmissivity of waves is concerned, by a single straight line, provided that the velocity of sound c' in the new straight duct is equal to $c' = c \cdot z_n$ (as if containing some medium other than air). For very low frequencies and bends of arbitrary sharpness, the phase velocity will be calculated by methods of Ref. 1. For higher frequencies it will be convenient to use Fig. 7. Experimental information on the transmissivity of bends may be found in Cummings' work. He gives data on the transmission coefficient of bends of a = 1.59 and a = 10.2. The first bend tested in the frequency parameter range of $1.06 < kR_1 < 5.3$ had the transmission coefficient $\alpha_t = 1$ throughout the frequency range, which checks very well against the analytical result ($\alpha_t = 1.0 - 4\times10^{-6}$). The second bend, tested in the frequency parameter range $0.068 < kR_1 < 0.34$, had a transmissivity slightly less than 1, 0.975 on the average. This again checks well with the approximate theoretical result ($\alpha_t = 0.994$) for $kR_1 = 0.068$ with $z_n = 1.17$. Furthermore, in the case of the second bend, at $kR_1 = 0.2$ Cummings obtained $\alpha_t = 1$. This could be anticipated because at this frequency parameter $c = c'$ and $z_n = 1$. The selectively bumpy experimental curve may be explained by the high probability of frequency controlled evanescent waves in the zone of measurements and by a lack of uniformity in the transmission characteristic.

The natural oscillations in ducts containing cylindrical bends may be best studied on systems open at one end and closed on the other. As a starting point, we may write that the input point impedance of a straight duct with a closed end (with the far end impedance infinite) and with negligible attenuation becomes a pure reactance

$$\chi = -j\rho c \cot (kl)$$

Now, the well known equations given in some texts, for instance Ref. 7, for natural frequencies for a system of two straight ducts of lengths l_1 and l_2, of identical cross section, and connected in series, are:

$$\tan (kl_1) = \cot (kl_2) \qquad \text{for a closed far end}$$

$$\tan (kl_1) = -\tan (kl_2) \qquad \text{for an open far end}$$

which will be satisfied if

$$k(l_1 + l_2) = \begin{cases} (2n+1)\pi/2 & \text{open duct} \\ \pi n & \text{closed duct} \end{cases}$$

Now, if we replace duct number 2 by a bend, the equations for a closed end system will be $\tan(kl) = \cot(\nu\theta)$ and $\theta + kl = (2n+1)\pi/2$ where θ, in radians, refers to the angular position of the closed end of duct number 2. For very low frequencies, $\nu = kR_1 = kR_m$ and s/R_m where R_m is the radius of the bend's centerline and s is the length of the bend along this center line. Consequently $\nu\theta = ks$ which reduces the expression for the bend to an expression for a straight line. For higher frequencies, the matter is not so simple. A more general expression must be used which for a closed-end system is $\tan(kl_1) = X\mathrm{ctg}(ykl_1)$ where $y = l_1/l_2$ and X is some ratio of the acoustic specific impedances z_c of the two elements in series in a ducting system. Expression $\tan(kl_1) \cdot \tan(ykl_1) = X$, for $y = 1$, yields $\tan(kl_1) = \sqrt{X}$; in general, however, a set of points must be found to satisfy this equation. We shall remember that for a narrow duct, up to and including $a = 1.5$, $X \cong 1$ and the solution is straightforward.

CONCLUDING REMARKS

Propagating and non-propagating modes of waves in the acoustic frequency range have been examined using a model, a system consisting of straight and curved duct sections. A method has been presented for determination of the non-propagating, evanescent modes generated at junctions, and of reflections due to impedance mismatch at junctions. It was indicated that each particular case of ducting must be examined separately. Only general formulations can be given for all shapes of ducting. Numerical values depend on the specific application and cannot be predicted without close analysis.

REFERENCES

1. Rostafinski, W. (1972). "On Propagation of Long Waves in Curved Ducts," J. Acoust. Soc. Am. 52, 1411-1420.

2. Rostafinski, W. (1974). "Analysis of Propagation of Waves of Acoustic Frequencies in Curved Ducts," J. Acoust. Soc. Am. 56, 11-15.

3. Cummings, A. (1974). "Sound Transmission in Curved Duct Bends," J. Sound and Vibration 35, 451, 477.

4. Rostafinski, W. (1974). "Transmission of Wave Energy in Curved Ducts," J. Acoust. Soc. Am. 56, 1005-1007.

5. Boole, G. (1844). "On the General Method of Analysis," Phil. Trans. Roy. Soc. 225-282.

6. Buckens, F. (1963). "Tables of Bessel Functions of Imaginary Order," Dept. of Applied Mechanics and Mathematics, Univ. of Louvain, Belgium.

7. Rschevkin, S. N. (1953). The Theory of Sound. (The Macmillan Co., New York).

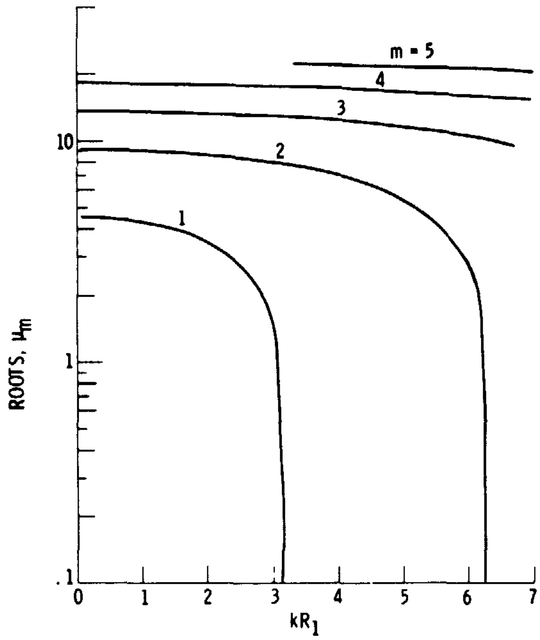

Fig. 1. - First five roots for duct with a = 2; in range of frequency parameters kR_1.

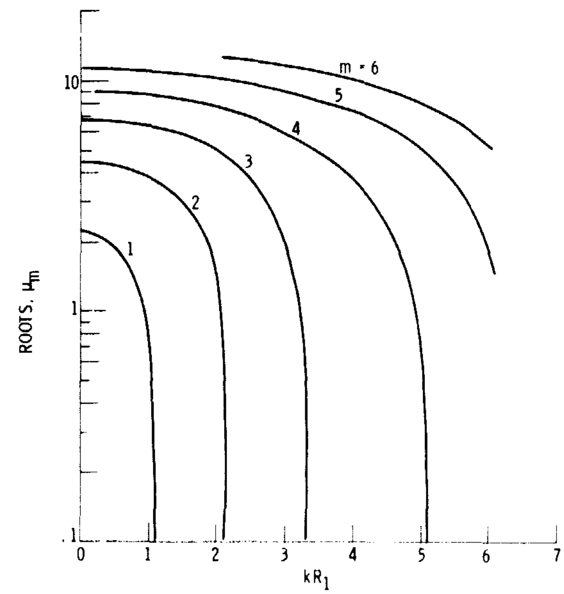

Fig. 2. - First six roots for duct with a = 4; in range of frequency parameter kR_1.

PRECEDING PAGE BLANK NOT FILMED

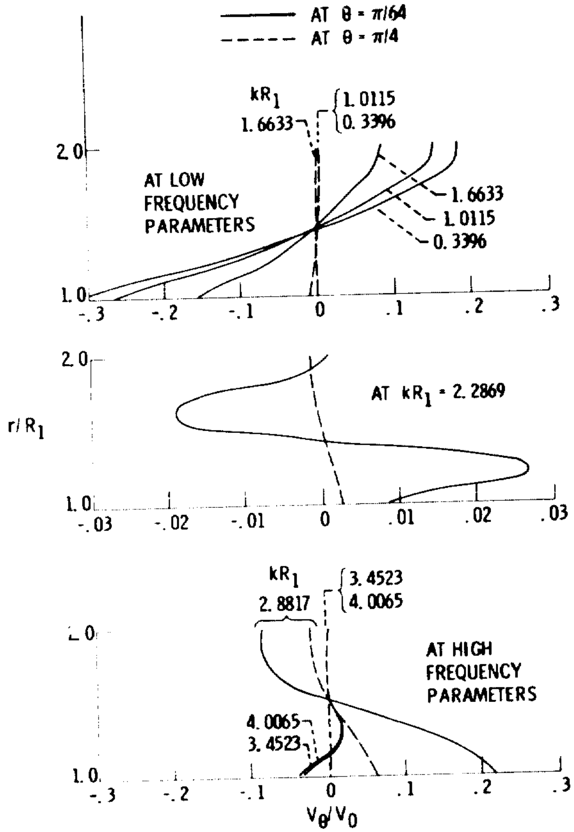

Fig. 3. - Nonpropagating tangential vibrational velocities.

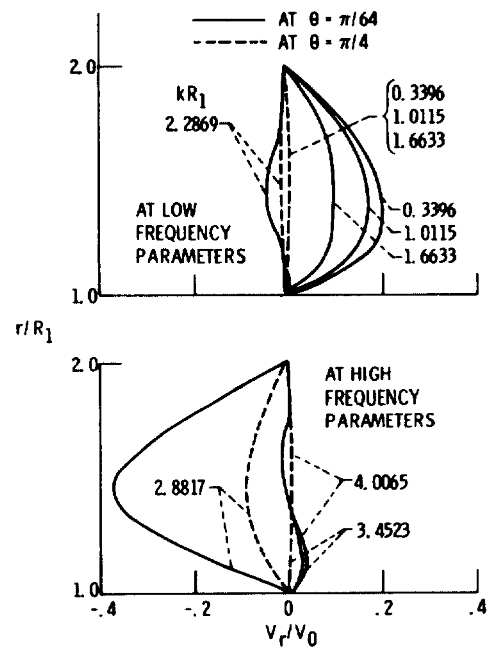

Fig. 4. - Nonpropagating radial vibrational velocities.

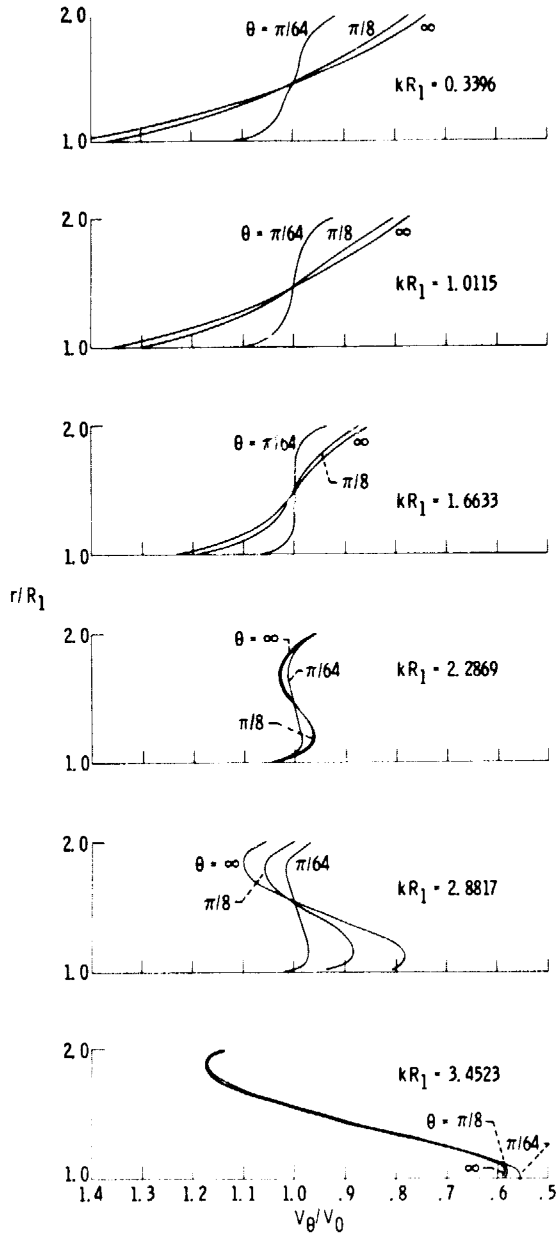

Fig. 5. - Tangential vibrational velocities.

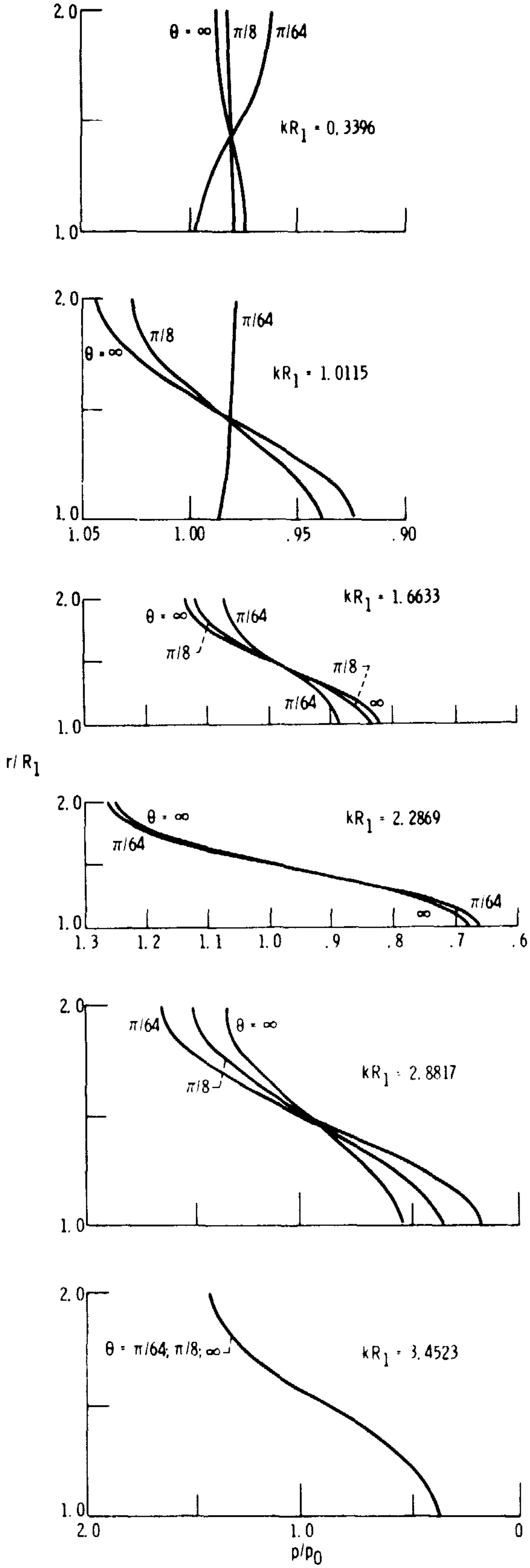

Fig. 6. - Acoustic pressure in bends.

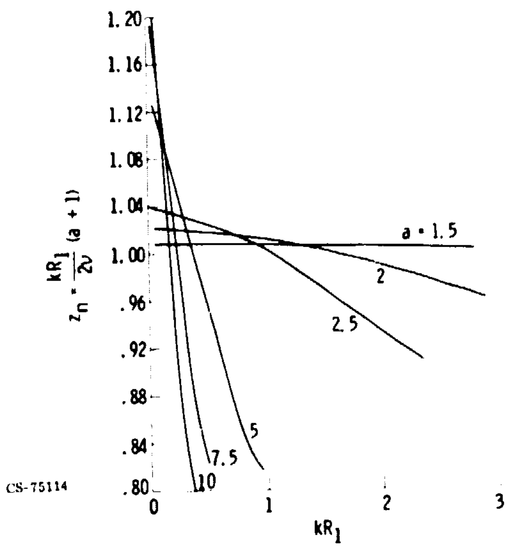

Fig. 7. - Dimensionless impedance of bends.